RECENT ADVANCES ON THE THEORETICAL AND NUMERICAL INVESTIGATIONS OF THE CONSTRAINED AEOLOTROPIC PIPE PROBLEM

Adair R. Aguiar,
aguiarar@sc.usp.br
Escola de Engenharia de São Carlos, Universidade de São Paulo
Av. Trabalhador Sãocarlense, 400, 13566-590, São Carlos, SP – Brazil
Roger L. Fosdick
fosdick@aem.umn.edu
Institute of Technology, University of Minnesota
110 Union Street SE, 55455-0153, Minneapolis, MN – USA
Jesús A. G. Sánchez
jesusg@sc.usp.br
Escola de Engenharia de São Carlos, Universidade de São Paulo
Av. Trabalhador Sãocarlense, 400, 13566-590, São Carlos, SP – Brazil

Abstract. *We have found a closed form expression for a minimizer of the total potential energy of a circular homogeneous and aeolotropic pipe in the context of a constrained minimization theory that preserves injectivity. The pipe is in a state of plane deformation, is fixed at its inner surface, and is radially compressed along its outer surface. To find the closed form expression, we have assumed that the displacement field is radially symmetric with respect to the center of the pipe. In this case, the only non-zero component of the displacement field is the radial one, which is a function of the radius only. In the special case of a solid circular cylinder, a full bi-dimensional numerical investigation carried out elsewhere has shown that another solution, which is not radially symmetric, is possible. This numerical solution is quite different from the radially symmetric solution. In this work, some recent results concerning both the analytical and numerical investigations of the constrained pipe problem are presented.*

Keywords: *Aeolotropic elasticity, Finite element method, Constrained minimization theory, Nonlinear programming*

1. INTRODUCTION

There are well-posed problems in the classical linear theory of elasticity whose closed form solutions allow material overlapping to occur. Typically, problems of this kind involve some sort of singularity, and strains exceeding a level acceptable from the point of view of a linear theory occur around the singular points (Aguiar, 2006a; Aguiar & Fosdick, 2001).

We consider a two-dimensional problem in classical linear elasticity for which material overlapping occurs in the absence of singularities. The problem concerns the equilibrium of a circular homogeneous and aeolotropic pipe, which is in a state of plane deformation perpendicular to the axis of the pipe, is fixed at its inner surface, and is radially compressed along its outer surface by a uniformly distributed normal force p. The requirement that the displacement field be radially symmetric with respect to the center of the pipe allows the derivation of a closed form solution that predicts overlapping of material at the inner surface of the linear elastic pipe when the radial compressive force p becomes larger than a critical load p_1, which is small.

One possible way to prevent the anomalous self-intersection behavior is proposed by Fosdick & Royer-Carfagni (2001). It combines the linear theory with the imposition of a local injectivity constraint through a Lagrange multiplier technique. These authors investigate the problem of minimizing the total potential energy $\mathcal{E}$ of classical linear elasticity on an admissible set $\mathcal{A}_\varepsilon$ of vector-valued functions $\mathbf{v}$ that satisfy the injectivity constraint $\det(\mathbf{1}+\nabla\mathbf{v}) \geq \varepsilon > 0$ for a sufficiently small $\varepsilon \in \mathbb{R}$. In particular, they show the existence of a solution for the constrained minimization problem in two dimensions and apply the results of their constrained minimization theory in the analysis of a *disk problem*, which corresponds to the *pipe problem* described above when the inner radius is zero. They show that two regions coexist inside the disk for moderate values of p: a central region for which $\det(\mathbf{1}+\nabla\mathbf{v}) = \varepsilon$ and an outer annular region for which $\det(\mathbf{1}+\nabla\mathbf{v}) \geq \varepsilon$. If p becomes too large, we have that $\det(\mathbf{1}+\nabla\mathbf{v}) = \varepsilon$ in the whole disk region.

We use the constrained theory of Fosdick & Royer-Carfagni (2001) to find a solution of the pipe problem that respects the injectivity constraint. Here, no region with $\det(\mathbf{1}+\nabla\mathbf{v}) = \varepsilon$ exists for $p < p_1$, where p_1 is the critical load mentioned above. For larger, but still moderate, values of p, we have both an annular region surrounding the inner boundary surface of the pipe for which $\det(\mathbf{1}+\nabla\mathbf{v}) = \varepsilon$ and an outer annular region for which $\det(\mathbf{1}+\nabla\mathbf{v}) \geq \varepsilon$. For even larger values of p, we then have that $\det(\mathbf{1}+\nabla\mathbf{v}) = \varepsilon$ in the whole disk region.

Recently, Fosdick, Freddi, and Royer-Carfagni (2007) have considered the full bidimensional disk problem, where we recall from above that the disk corresponds to a pipe with zero inner radius, and have shown numerical results which indicate that the radial symmetry may not persist for all values of the shear elastic modulus. Because the constrained theory is nonlinear, there are values of the shear modulus for which bifurcation from radial symmetry to non-radial symmetry is a definite possibility.

Aguiar (2004, 2006a) assume radial symmetry to solve different classes of constrained problems and present a finite element approach to find numerical approximations to these problems. The approach is based on an *interior penalty formulation*, which consists of replacing the total potential energy $\mathcal{E}$ of an elastic body by a penalized functional $\mathcal{E}_\gamma = \mathcal{E} + Q/\gamma$, where γ is an arbitrary positive number and Q is a penalty functional defined on a constraint set $\mathcal{A}_\varepsilon$ of displacement fields $\mathbf{v}$ that satisfy both the injective constraint $\det\left(\mathbf{1}+\nabla\mathbf{v}\right) \geq \varepsilon > 0$ and essential boundary conditions on the external surface of the body. The penalty functional is non-negative on $\mathcal{A}_\varepsilon$, satisfies $Q[\mathbf{v}] \to \infty$ as $\mathbf{v}$ approaches the boundary of $\mathcal{A}_\varepsilon$, and is designed so that minimizers of $\mathcal{E}_\gamma$ lie in the interior of the constraint set $\mathcal{A}_\varepsilon$. Thus, the interior penalty formulation consists of finding $\mathbf{u}_\gamma \in \mathcal{A}_\varepsilon$ that minimizes the penalized functional $\mathcal{E}_\gamma$ over the constraint set $\mathcal{A}_\varepsilon$. The solution of the original constrained minimization problem is obtained as the limit function of a sequence of minimizers of $\mathcal{E}_\gamma$, parameterized by γ, as $\gamma \to \infty$.

Aguiar (2006b) and Aguiar et al (2008) present a different finite element approach, which is based on an *exterior penalty formulation*. It also consists of replacing $\mathcal{E}$ by a penalized functional $\mathcal{E}_\delta = \mathcal{E} + \mathcal{P} / \delta$, where now δ is an arbitrary small number and $\mathcal{P}$ is a penalty functional defined on a set $\mathcal{A}$ of displacement fields that is only required to satisfy the essential boundary conditions. Clearly, $\mathcal{A}_\varepsilon \subset \mathcal{A}$. The penalty functional is non-negative on $\mathcal{A}$ and satisfies $\mathcal{P}[\mathbf{v}] \to 0$ as $\mathbf{v}$ approaches the boundary of $\mathcal{A}_\varepsilon$. Thus, the exterior penalty formulation consists of finding $\mathbf{u}_\delta \in \mathcal{A}$ that minimizes the penalized functional $\mathcal{E}_\delta$ over the set $\mathcal{A}$. The solution of the original constrained minimization problem is obtained as the limit function of a sequence of minimizers of $\mathcal{E}_\delta$, parameterized by δ, as $\delta \to 0$.

Aguiar (2007) applies both penalty formulations in the analysis of the constrained disk problem considered by Fosdick and Royer (2001). In particular, he constructs convergent sequences of minimizers for either increasing values of γ or decreasing values of δ and show numerically that the resulting limit functions are the same for a given characteristic length of the finite element. We recall from the exposition above that the solution of the corresponding unconstrained problem yields not only self-intersection of material, but also singular stresses and strains at the center of the disk. In this work, we apply both penalty formulations in the analysis of the constrained pipe problem. In this way, we investigate the self-intersection behavior without the coupling effect of the singular stresses and strains. Results presented here first appeared in Aguiar et al (2008).

In Sections 2 and 3 we present some results concerning the compressed pipe problem in the context of the unconstrained and the constrained theories, respectively. In Section 4 we present both the interior and the exterior penalty formulations of the constrained pipe problem. These formulations yield numerical schemes that are simple to implement and can be applied in the numerical solution of problems in any dimension. In Section 5 we compare the numerical results obtained from the solutions of the corresponding discrete problems with analytical results obtained from the closed form solution of the constrained minimization problem considered in Section 3.

2. THE UNCONSTRAINED PIPE PROBLEM

In classical linear elasticity, the pipe problem described in Section 1 is two-dimensional so that, relative to the usual orthonormal cylindrical basis $(\mathbf{e}_\rho, \mathbf{e}_\theta)$, the pipe cross-section occupies the region $\mathcal{B} \equiv \left\{ \mathbf{x} = \rho\, \mathbf{e}_\rho : \rho_i \le \rho \le \rho_e \right\}$, where ρ_i and ρ_e are, respectively, the inner radius and the outer radius of the pipe. Also, the components of the stress and strain tensors are related to each other by the linear constitutive relations

$$\sigma_{\rho\rho} = c_{11}\varepsilon_{\rho\rho} + c_{12}\varepsilon_{\theta\theta}, \qquad \sigma_{\theta\theta} = c_{12}\varepsilon_{\rho\rho} + c_{22}\varepsilon_{\theta\theta}, \qquad \sigma_{\rho\theta} = 2G\varepsilon_{\rho\theta}, \tag{1}$$

where $c_{11} > 0$, $c_{22} > 0$, and $G > 0$ are elastic constants that satisfy $c_{11}c_{22} - c_{12}{}^2 > 0$. Since uniqueness is guaranteed in classical linear elasticity, the displacement field must be radially symmetric with respect to the center of the pipe, i.e., $\mathbf{u}(\rho,\theta) = u(\rho)\mathbf{e}_\rho$. Thus, the strain components take the form

$$\varepsilon_{\rho\rho} = u'(\rho), \qquad \varepsilon_{\theta\theta} = u(\rho)/\rho, \qquad \varepsilon_{\rho\theta} = 0, \tag{2}$$

where $(\cdot)' = d(\cdot)/d\rho$. In view of both Eq. (1) and Eq. (2), the equilibrium equations in the absence of body force yield

$$u'' + \frac{u'}{\rho} - \kappa^2 \frac{u}{\rho^2} = 0 \quad \text{in } (\rho_i, \rho_e), \qquad \kappa = \sqrt{\frac{c_{22}}{c_{11}}}. \tag{3}$$

The solution of this ordinary differential equation that satisfies the displacement and traction boundary conditions

$$u(\rho_i) = 0, \qquad \sigma_{\rho\rho} = c_{11}u' + c_{12}\frac{u}{\rho} = -p \qquad \text{on } \rho = \rho_e, \tag{4}$$

respectively, is given by

$$u(\rho) = -\frac{\rho_i}{2\kappa}\left[\left(\frac{\rho}{\rho_i}\right)^{\kappa} - \left(\frac{\rho}{\rho_i}\right)^{-\kappa}\right]\frac{p}{p_1} \qquad \text{for } \rho_i \le \rho \le \rho_e, \tag{5}$$

where

$$p_1 = \frac{\rho_i}{\rho_e}\left[(\kappa - \mu_\theta)\left(\frac{\rho_i}{\rho_e}\right)^{\kappa} + (\kappa + \mu_\theta)\left(\frac{\rho_i}{\rho_e}\right)^{-\kappa}\right]\frac{c_{11}}{2\kappa} > 0, \qquad \mu_\theta \equiv \frac{c_{12}}{c_{11}}. \tag{6}$$

In the limit, as $\rho_i \to 0$, we obtain from Eq. (5) together with Eq. (6) the solution of the solid disk problem presented by Lekhnitskii (1968).

It follows from Eq. (5) that both $u'(\rho) < 0$ and $u''(\rho) > 0$ for $\rho \in (\rho_i, \rho_e)$ and for $0 < \kappa < 1$, which means that u is a convex function of ρ and that its derivative u' is a monotonically increasing function of ρ with its minimum at $\rho = \rho_i$. Since our main interest in this work is to analyze the sign of the Jacobian determinant

$$J \equiv \det(\mathbf{1} + \nabla\mathbf{v}) = (1 + u')\left(1 + \frac{u}{\rho}\right), \tag{7}$$

we see from Eq. (5) - Eq. (7) that a critical value of the load p that yields $J < 0$ is obtained from $u'(\rho) = -1$ and is given by $p = p_1$, where p_1 is defined by Eq. (6.a). Clearly, we may have p_1, and hence p, as small as we wish by decreasing the value of ρ_i and still have bounded stresses and strains everywhere. In this work, we are only concerned with $0<\kappa<1$.

Similarly, we can show that $u(\rho)/\rho$ is convex at $\rho=\rho_i$ and, for $0<\kappa<1$, has a unique minimum at a point with radius $\rho_m>\rho_i$. The critical value of p for which $u(\rho_m)/\rho_m=-1$ is given by

$$p_2=(1-\kappa)\left(\frac{1+\kappa}{1-\kappa}\right)^{\left(\frac{1+\kappa}{2\kappa}\right)} p_1, \tag{8}$$

which is greater than p_1 for $0<\kappa<1$. In fact, $p_2>2p_1$.

To avoid crushing of the outer surface into the inner surface of the pipe, we must have $-u(\rho_e)/\rho_e=1-\rho_i/\rho_e$, which, because of Eq. (5), imposes the restriction

$$p<p_c\equiv\left[\frac{2(1-\eta)\eta^{\kappa-1}}{1-\eta^{2\kappa}}\right]p_1, \qquad \eta\equiv\left(\frac{\rho_i}{\rho_e}\right). \tag{9}$$

Since $p_c\gg p_1$ for both $\rho_i\ll\rho_e$ and $\kappa<1$, we conclude from the above that local injectivity is lost for non-zero values of p that are small compared to the critical value p_c.

Thus, for $0<\kappa<1$, the classical solution has no physical meaning and therefore should be rejected as a viable solution. In the next section, we use the constrained minimization theory of Fosdick & Royer-Carfagni (2001) to derive a solution for the pipe problem described in Section 1 that is everywhere injective, i.e., a solution for which $J>0$.

3. THE CONSTRAINED PIPE PROBLEM

Recall from Section 2 that $\mathcal{B}$ is the region occupied by the pipe cross-section. Here, we consider that $\mathcal{B}\equiv\mathcal{B}_=\cup\mathcal{B}_>$, where $\mathcal{B}_=\equiv\left\{\mathbf{x}=\rho\,\mathbf{e}_\rho:\det(\mathbf{1}+\nabla\mathbf{u})=\varepsilon,\rho_i\le\rho\le\rho_a\right\}$, and $\mathcal{B}_>\equiv\left\{\mathbf{x}=\rho\,\mathbf{e}_\rho:\det(\mathbf{1}+\nabla\mathbf{u})\ge\varepsilon,\rho_a\le\rho\le\rho_e\right\}$ for both $\varepsilon>0$ and some $\rho_a\in(\rho_i,\rho_e)$ yet to be determined. Assuming that the displacement field is radially symmetric with respect to the center of the pipe in a state of plane strain[1], i.e., that $\mathbf{u}(\rho,\theta)=u(\rho)\mathbf{e}_\rho$, we find that the necessary first variation conditions for the existence of a minimizer are satisfied by

$$u(\rho)=\begin{cases} g(\rho)-\rho, \qquad g(\rho)\equiv\sqrt{\left(\rho^2-\rho_i^{\,2}\right)\varepsilon+\rho_i^{\,2}}, & \rho\in(\rho_i,\rho_a), \\ \dfrac{\rho_a}{2\kappa}\left[\beta_1\left(\dfrac{\rho}{\rho_a}\right)^{\kappa}+\beta_2\left(\dfrac{\rho}{\rho_a}\right)^{-\kappa}\right], & \rho\in(\rho_a,\rho_e), \end{cases} \tag{10}$$

where

[1] Recently, Fosdick, Freddi, and Royer-Carfagni (2007) have considered the full bidimensional disk problem, for which $\rho_i=0$, and have shown numerical results that indicate that this symmetry may not persist for all values of the elastic constant G in Eq. (1).

$$\beta_1 \equiv -(1+\kappa) + \frac{\kappa g(\rho_a)}{\rho_a} + \frac{\varepsilon \rho_a}{g(\rho_a)}, \qquad \beta_2 \equiv 1-\kappa + \frac{\kappa g(\rho_a)}{\rho_a} - \frac{\varepsilon \rho_a}{g(\rho_a)}, \tag{11}$$

and ρ_a satisfies the algebraic equation

$$0 = r(\zeta) \equiv s(\zeta;\kappa) + s(\zeta;-\kappa) + \frac{p}{c_{11}}, \qquad \zeta \equiv \frac{\rho_a}{\rho_e}. \tag{12}$$

In Eq. (12),

$$s(\zeta;\kappa) \equiv \left(\frac{\kappa+\mu_\theta}{2\kappa}\right)\zeta^{1-\kappa}\left[-(1+\kappa) + \frac{\kappa \hat{g}(\zeta)}{\zeta} + \frac{\varepsilon\zeta}{\hat{g}(\zeta)}\right] \tag{13}$$

is a function of ζ parameterized by κ, where $\hat{g}(\zeta) \equiv \sqrt{(\zeta^2 - \zeta_i^2)\varepsilon + \zeta_i^2}$ and $\zeta_i \equiv \dfrac{\rho_i}{\rho_e}$.

Notice from Eq. (12) together with Eq. (13) that $r(\zeta_i) = \left[p - (1-\varepsilon)p_1\right]/c_{11}$, where p_1 is given by Eq. (6). Notice also that $r(1) = p - p_0$, where $p_0 \equiv \left\{1 + \mu_\theta - \left[\dfrac{\varepsilon + \mu_\theta \hat{g}(1)^2}{\hat{g}(1)}\right]\right\}c_{11} > p_1$ since both ζ_i and $\varepsilon > 0$ are sufficiently small. Taking the derivative of r in Eq. (12), we obtain that $r'(\zeta)$ is negative, because $\kappa + \mu_\theta > 0$, $\kappa - \mu_\theta > 0$, and $\varepsilon > 0$ is sufficiently small. Thus, if $r(\zeta_i) < 0$, then $r(\zeta) = 0$ has no roots, which is consistent with results obtained in Section 2, according to which $p - p_1 < 0$ implies no self-intersection. If, on the other hand, both $r(\zeta_i) \geq 0$ and $r(1) \leq 0$, then there exists a unique $\zeta \in [0,1]$ that satisifies $r(\zeta) = 0$. In particular, if $p = (1-\varepsilon)p_1$, then $\zeta = \zeta_i$ and if $p = p_o$, $\zeta = 1$. Furthermore, if $p > p_o$, no $\zeta \in [\zeta_i, 1]$ exists that satisfies $r(\zeta) = 0$. In this case, $\rho_a = \rho_e$.

Using Eq. (10) together with Eq. (11) in Eq. (7), we can easily obtain an expression for J, which is positive everywhere in $[\rho_i, \rho_e]$. Thus, the solution given by Eq. (10) together with Eq. (11) describes the deformation of the pipe under radial pressure, which is both locally and globally injective.

In general, constrained minimization problems are highly nonlinear and require a numerical solution. In the next section we use a penalty method together with a standard finite element procedure to find an approximate solution of the constrained pipe problem. The numerical scheme forms the computational basis for the analysis of problems for which no symmetry considerations exist and is being applied in the approximate solution of full two-, or, three-dimensional problems.

4. THE PENALTY FORMULATION

The formulation presented here is general and applies to any bounded domain in $\mathbb{R}^2$ with smooth boundary. Thus, let $\mathcal{B} \subset \mathbb{R}^2$ be the undistorted natural reference configuration of a body. Points $\mathbf{x} \in \mathcal{B}$ are mapped to points $\mathbf{y} = \mathbf{f}(\mathbf{x}) \equiv \mathbf{x} + \mathbf{u}(\mathbf{x}) \in \mathbb{R}^2$, where $\mathbf{u}(\mathbf{x})$ is the displacement of $\mathbf{x}$. The boundary $\partial\mathcal{B}$ of $\mathcal{B}$ is composed of two non-intersecting parts, $\partial_1\mathcal{B}$ and $\partial_2\mathcal{B}$, $\partial_1\mathcal{B} \cup \partial_2\mathcal{B} = \partial\mathcal{B}$, $\partial_1\mathcal{B} \cap \partial_2\mathcal{B} = \varnothing$, such that $\mathbf{u}(\mathbf{x}) = \mathbf{0}$ for $\mathbf{x} \in \partial_1\mathcal{B}$ and such that a dead load traction field $\bar{\mathbf{t}}(\mathbf{x})$ is prescribed for $\mathbf{x} \in \partial_2\mathcal{B}$. In addition, a body force $\mathbf{b}(\mathbf{x})$ per unit volume of $\mathcal{B}$ acts on points $\mathbf{x} \in \mathcal{B}$.

Let

$$\mathcal{A} \equiv \left\{ \mathbf{v} : W^{1,2}(\mathcal{B}) \to \mathbb{R}^2 \mid \mathbf{v} = \mathbf{0} \text{ a.e. on } \partial_1\mathcal{B} \right\} \tag{14}$$

be the class of displacement fields that respect essential boundary conditions and let

$$\mathcal{A}_\varepsilon \equiv \left\{ \mathbf{v} : \mathcal{A} \to \mathbb{R}^2 \mid \det(\mathbf{1} + \nabla\mathbf{v}) \geq \varepsilon > 0 \right\} \tag{15}$$

be the class of admissible displacement fields. We suppose that $\varepsilon > 0$ in Eq. (15) is sufficiently small. We then consider the problem of minimum potential energy:

$$\min_{\mathbf{v}\in\mathcal{A}_\varepsilon} \mathcal{E}[\mathbf{v}], \qquad \mathcal{E}[\mathbf{v}] = \frac{1}{2} a(\mathbf{v},\mathbf{v}) - f(\mathbf{v}), \tag{16}$$

where

$$a(\mathbf{v},\mathbf{v}) = \int_{\mathcal{B}} \mathbb{C}[\mathbf{E}] \cdot \mathbf{E} \, \mathrm{d}\mathbf{x}, \qquad f[\mathbf{v}] \equiv \int_{\mathcal{B}} \mathbf{b} \cdot \mathbf{v} \, \mathrm{d}\mathbf{x} + \int_{\partial\mathcal{B}} \bar{\mathbf{t}} \cdot \mathbf{v} \, \mathrm{d}\mathbf{x}. \tag{17}$$

In Eq. (17), $\mathbb{C} = \mathbb{C}(\boldsymbol{x})$ is the elasticity tensor, assumed to be positive definite and totally symmetric, and $\mathbf{E} \equiv \left[\nabla\mathbf{v} + (\nabla\mathbf{v})^T \right] / 2$ is the infinitesimal strain tensor field. The functional $\mathcal{E}[\cdot]$ is the total potential energy of classical linear theory of elasticity.

Fosdick and Royer-Cafagni (2001) fully characterize the solutions of the minimization problem given by both Eq. (16) and Eq. (17). In particular, they show that there exists a solution to this problem and they derive first variation conditions for a minimizer $\mathbf{u} \in \mathcal{A}_\varepsilon$ of $\mathcal{E}[\cdot]$.

Aguiar (2006a) presents an *interior penalty functional formulation* of the minimization problem given by both Eq. (16) and Eq. (17), which consists of replacing the energy functional given by Eq. (16.b) by a penalized potential energy functional $\mathcal{E}_\gamma : \mathcal{A}_\varepsilon \to \bar{\mathbb{R}}$, $\bar{\mathbb{R}} \equiv \mathbb{R} \cup \{\infty\}$, of the form

$$\mathcal{E}_\gamma[\mathbf{u}] = \mathcal{E}[\mathbf{u}] + \frac{1}{\gamma} \mathcal{Q}[\mathbf{u}], \tag{18}$$

where $\gamma > 0$ is a penalty parameter and $Q : \mathcal{A}_\varepsilon \to \overline{\mathbb{R}}$ is a *barrier functional*, given by

$$Q[\mathbf{v}] = \int_{\mathcal{B}} \frac{1}{p(\mathbf{v})} d\mathbf{x}, \qquad p(\mathbf{v}) \equiv \det(1 + \nabla \mathbf{v}) - \varepsilon, \qquad \forall\, \mathbf{v} \in \mathcal{A}_\varepsilon. \tag{19}$$

Observe from Eq. (19) that Q is non-negative on $\mathcal{A}_\varepsilon$ and satisfies $Q[\mathbf{v}] \to \infty$ as $\mathbf{v}$ approaches the boundary of $\mathcal{A}_\varepsilon$. The interior penalty formulation consists of finding an admissible displacement field $\mathbf{u} \in \mathcal{A}_\varepsilon$ that minimizes the penalized potential $\mathcal{E}_\gamma[\cdot]$, i.e.,

$$\min_{\mathbf{v} \in \mathcal{A}_\varepsilon} \mathcal{E}_\gamma[\mathbf{v}] \;. \tag{20}$$

This is a constrained problem, and indeed the functional to be minimized is somewhat more complicated than the original energy functional given by Eq. (16.b). The advantage of considering this problem, however, is that we can use numerical procedures commonly employed in the numerical approximation of solutions of unconstrained problems.

On the other hand, an *exterior penalty functional formulation* of the minimization problem given by both Eq. (16) and Eq. (17) consists of replacing the energy functional given by Eq. (16.b) by a penalized potential energy functional $\mathcal{E}_\delta$ of the form

$$\mathcal{E}_\delta[\mathbf{u}] = \mathcal{E}[\mathbf{u}] + \frac{1}{\delta} \mathcal{P}[\mathbf{u}], \tag{21}$$

where $\delta > 0$ is a penalty parameter and $\mathcal{P} : \mathcal{A} \to \mathbb{R}$ is a *penalty functional*, which is non-negative in $\mathcal{A}$ and is designed so that $\mathcal{P}[\mathbf{v}]$ increases with the distance from $\mathbf{v}$ to the constraint set $\mathcal{A}_\varepsilon$. In this work, we consider

$$\mathcal{P}[\mathbf{v}] = \frac{1}{2} \int_{\mathcal{B}} \left[\max(0, -p(\mathbf{v}))\right]^2 d\mathbf{x} \;, \qquad \forall \mathbf{v} \in \mathcal{A}, \tag{22}$$

where $\max(0, -p) \equiv (-p + |p|)/2$, and $p(\mathbf{v})$ is given by Eq. (19.b). Clearly, $\mathcal{P}[\mathbf{v}] = 0$ if the injectivity constraint is satisfied; otherwise, $\mathcal{P}[\mathbf{v}] > 0$. The choice given by Eq. (22) for $\mathcal{P}$ leads to a discrete version of the penalized energy functional $\mathcal{E}_\delta$ that is continuous and differentiable everywhere. We then want to find an admissible displacement field $\mathbf{u}_\delta \in \mathcal{A}_\varepsilon$ that minimizes the penalized potential $\mathcal{E}_\delta[\cdot]$, i.e.,

$$\min_{\mathbf{v} \in \mathcal{A}} \mathcal{E}_\delta[\mathbf{v}]. \tag{23}$$

This is an unconstrained problem, which has the advantage of yielding discrete minimization problems that can be solved by classical unconstrained nonlinear programming techniques.

In the next section we use both the interior and the exterior penalty formulations together with a standard finite element technique and a classical nonlinear programming method[2] to find the solution of the constrained pipe problem presented in Section 3.

5. NUMERICAL RESULTS

We have normalized all lengths by setting $\rho_e = 1$, where we recall from Section 2 that ρ_e is the outer radius of the pipe. Furthermore, in dimensionless units, the inner radius of the pipe is $\rho_i = 0.001$, the applied load on the outer surface of the pipe is $p = 500$, and the elastic constants are $c_{11} = 10^5$, $c_{22} = 10^3$, $c_{12} = 10^3$, which, in view of Eq. (3.b), yield $\kappa = 0.1 < 1$. We then have from Eq. (6) that $p_1 = 0.00132$, from Eq. (8) that $p_2 = 0.00359$, and from Eq. (9) that $p_c = 1.76913$. As observed in Section 2, $p_c >> p_2 > 2p_1$. Also, we take $\varepsilon = 0.1$ for the lower bound of the injectivity constraint. The radius of the core subregion $\mathcal{B}_=$, where the constraint is active, is obtained from both Eq. (12) and Eq. (13) and is given by $\rho_a \cong 0.00554$.

In Fig. 1 we show curves for the radial deformation $1 + u'(\rho)$, the tangential deformation $1 + u(\rho)/\rho$, and the Jacobian determinant J, which is given by Eq. (7), versus the radius ρ in the interval (0.001, 0.010) for the unconstrained pipe problem presented in Section 2. Observe from this figure that the radial deformation is monotonically increasing and is zero at $\alpha_1 \cong 0.00381$. Observe also that the tangential deformation is zero at both $\alpha_2 \cong 0.00148$ and $\alpha_3 \cong 0.00784$. This is in agreement with our analysis in Section 2, since $p > p_2$. As a result, we obtain from Eq. (7) that J is positive in the interval $(0.00784, 1)$, negative in the interval $(0.00381, 0.00784)$, positive again in the interval $(0.00148, 0.00381)$, and negative again in the interval $(0.001, 0.00148)$. Although the positive values of J in the interval $(0.00148, 0.00381)$ have no physical meaning, they represent eversion of material taking place in both radial and tangential directions.

In Fig. 2 we show the Jacobian determinant J versus the radius ρ in the interval (0.001, 0.010) for both the unconstrained and the constrained pipe problems presented in Sections 2 and 3, respectively. Observe from this figure that J for the constrained problem, which is represented by the solid line, is positive everywhere. In particular, it is constant and equals to $\varepsilon = 0.1$ in the interval $(0.001, 0.00554)$.

In Fig. 3 we show curves representing both exact analytical solutions and numerical solutions. The numerical solutions were obtained with either the interior penalty formulation using a large value of γ or the exterior penalty formulation using a small value of δ. The solid line corresponds to the solution of the constrained pipe problem, given by Eq. (10) – Eq. (13), and the dash-dotted line corresponds to numerical solutions of the constrained pipe problem for an increasing number of finite elements (480, 960, …, 7680 elements). Observe from Fig. 3.a that both the exact and the numerical solutions of the constrained problem are indistinguishable and from Fig. 3.b, which corresponds to a zoom in a neighborhood of $\rho_a \cong 0.00554$, that the sequence of numerical solutions obtained with increasing number of finite elements converges to the constrained exact solution. We also show in Fig. 3.a the unconstrained exact solution, which is given by both Eq. (5) and Eq. (6) and is represented by the dashed line. By comparing this line with the solid line, we conclude that the imposition of

[2] Details of the numerical scheme for the interior penalty formulation are presented in Aguiar (2006a).

the injective constraint has the effect of stiffening the pipe. Similar conclusions are reached by Aguiar (2006a) and Fosdick and Royer-Carfagni (2001) in their treatment of radially symmetric constrained problems.

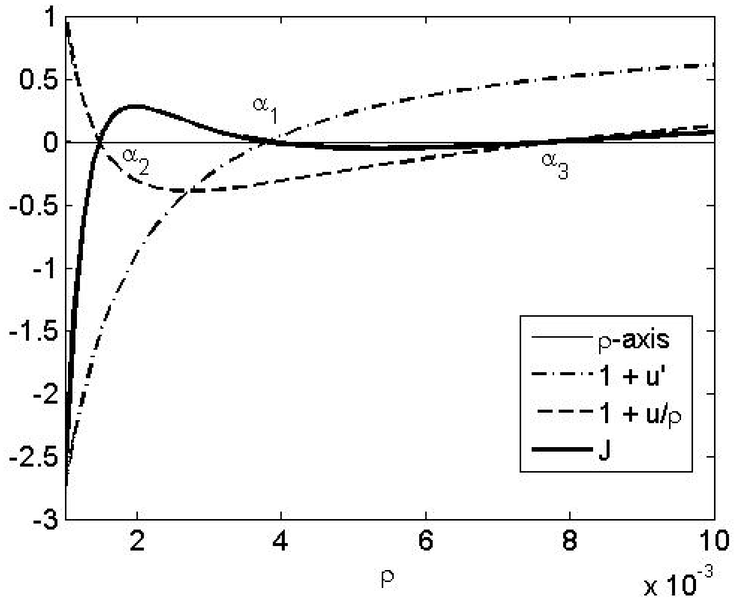

Figure 1. Radial deformation (-.-), tangential deformation (---), and the Jacobian determinant (__) versus radius ρ for the unconstrained pipe problem.

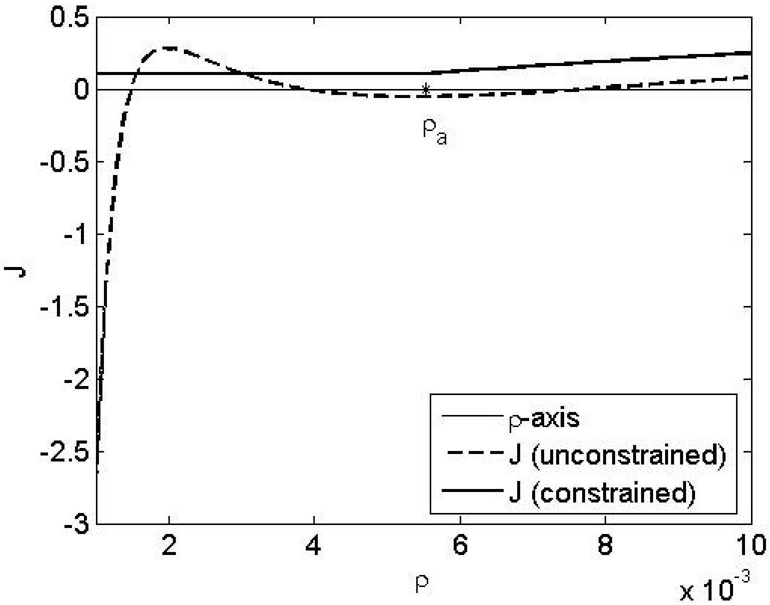

Figure 2. The Jacobian determinant J versus radius ρ for both the unconstrained (---) and the constrained (__) pipe problems.

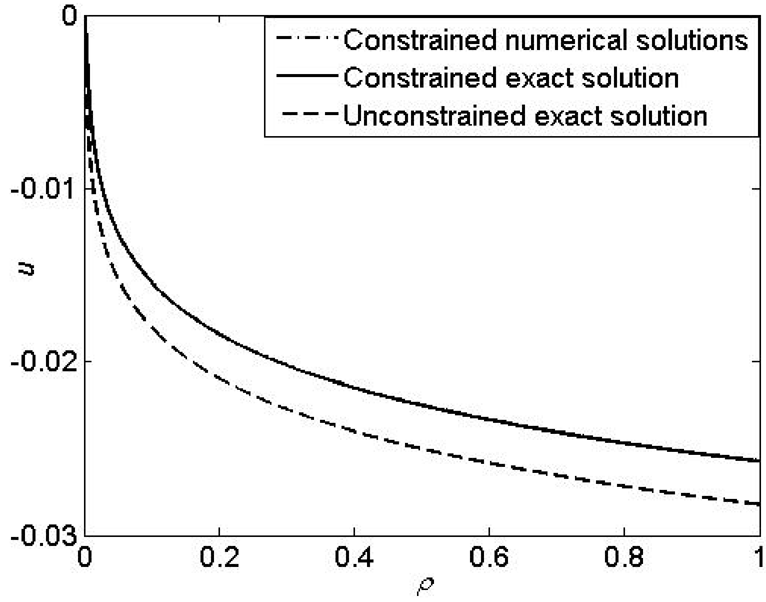

(3.a) Entire interval (0.001, 1).

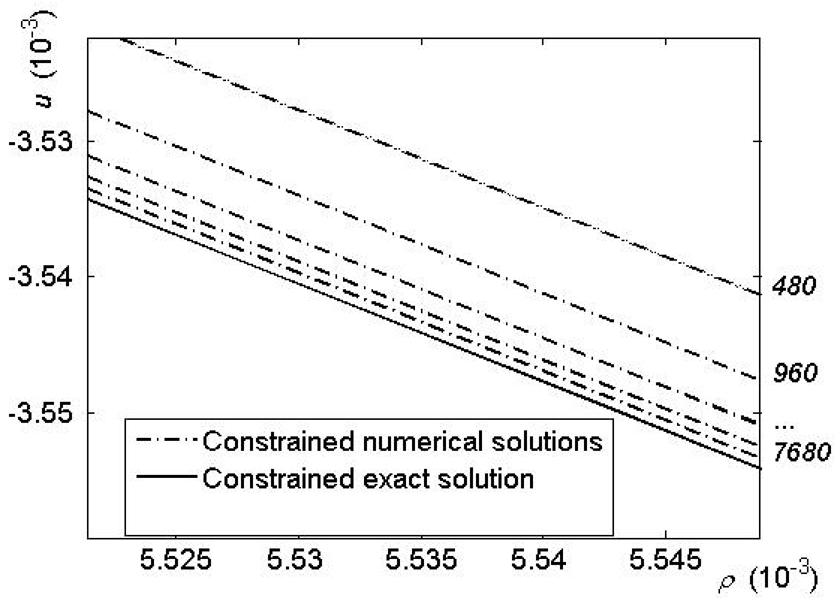

(3.b) Zoom in a neighborhood of $\rho_a \cong 0.00554$.

Figure 3. Radial displacement u versus radius ρ for the constrained pipe problem for either large γ or small δ and for an increasing number of finite elements.

In Fig. 4 we show the determinant of the deformation gradient, J, calculated from both the exact solution of the constrained problem, represented by the solid line, and the corresponding numerical approximations, obtained with increasing values of either γ or $1/\delta$ and represented by dash-dotted lines, for the most refined mesh of 7680 elements. Figures 4.a and 4.b refer to the approximations J_h obtained with, respectively, the interior and the exterior penalty formulations. Observe from both figures that J_h converges to a limit function as the penalty parameter is enforced in each case, i.e., as $\gamma \to \infty$ in Fig. 4.a and as $\delta \to 0$ in Fig. 4.b. Observe from Fig. 4.b that, in the interval (0.001, 0.00554), the approximations u_h of the minimizer u lie in the exterior of the set $\mathcal{A}_\varepsilon$ for large δ since, in this case, $J_h < \varepsilon$. Nevertheless, contrary to what one might expect, as $\delta \to 0$, the sequence of approximations $\{u_h\}$ converges to a limit function that belongs to the constrained set $\mathcal{A}_\varepsilon$.

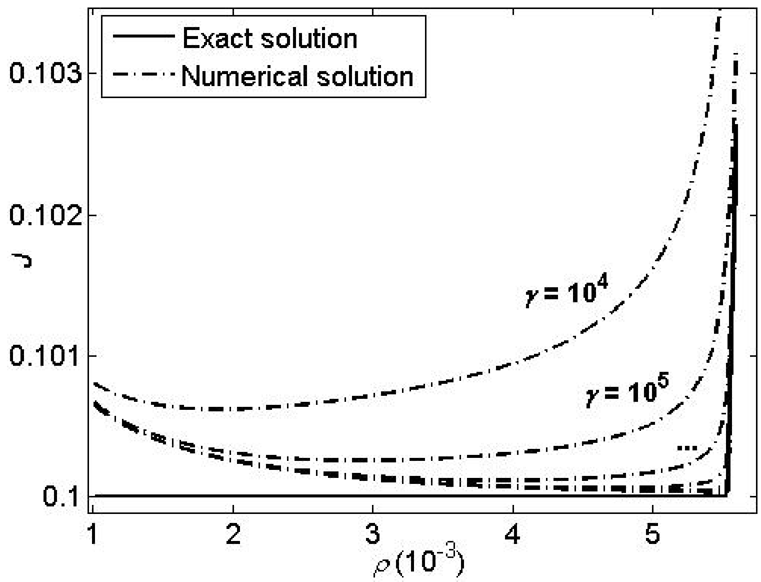

(4.a) Interior Penalty Formulation.

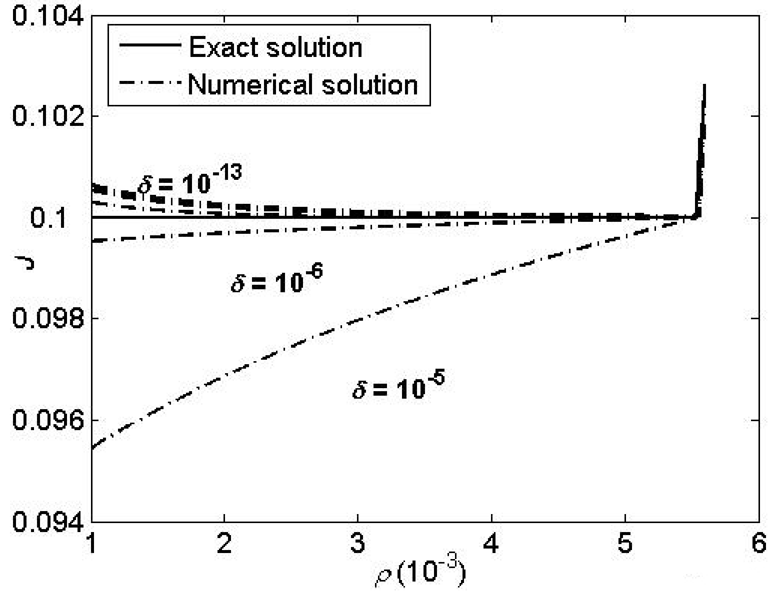

(4.b) Exterior Penalty Formulation.

Figure 4. Jacobian determinant J versus radius ρ for a large number of finite elements (7680 elements) and for increasing values of both (a) γ and (b) $1/\delta$.

Acknowledgements

The authors wish to acknowledge FAPESP (Fundação de Amparo à Pesquisa do Estado de São Paulo), Proc. No. 2007/03753-9, and the University of Minnesota Supercomputing Institute (UMSI) for their support of this research.

REFERENCES

Aguiar, A.R., Fosdick, R.L., & Sánchez, J.A.G., 2008. A Study of Penalty Formulations Used in the Numerical Approximation of a Radially Symmetric Elasticity Problem. *Journal of Mechanics of Materials and Structures*. Accepted for publication.

Aguiar, A.R., 2007. A Comparative Study of Penalty Formulations in Elasticity. In: Solid Mechanics in Brazil 2007 (MECSOL 2007), São Paulo, SP, March 6.

Aguiar, A.R., 2006a. Local and Global Injective Solution of the Rotationally Symmetric Sphere Problem. *Journal of Elasticity*, **84**, 99-129.

Aguiar, A.R., 2006b. An Exterior Penalty Method to Prevent Material Overlapping in Elasticity. In: *Iberian Latin American Congress on Computational Methods in Engineering (XXVII CILAMCE), Belém, PA, September 06.*

Aguiar, A.R., 2004. A Numerical Treatment of Material Overlapping in Elasticity. In: *Iberian Latin American Congress on Computational Methods in Engineering (XXV CILAMCE),* Mar Hotel, Recife, PE, November 11.

Aguiar, A.R. & Fosdick, R.L., 2001. Self-intersection in elasticity. *Int. J. Solids Structures*, **38**, 4797-4823.

Fosdick, R.L., Freddi, F., & Royer-Carfagni, G., 2007. Bifurcation instability in linear elasticity with the constraint of local injectivity. Journal of Elasticity, **90**, 99-126.

Fosdick, R.L. & Royer-Carfagni, G., 2001. The Constraint of Local Injectivity in Linear Elasticity Theory. *Proc. R. Soc. Lond. A*, **457**, 2167-2187.

Lekhnitskii, S. G., 1968. *Anisotropic Plates*. New York: Gordon and Breach Science Publishers.